Environmental Earth Sciences (2018) 77:516
https://doi.org/10.1007/s12665-018-7696-8

ORIGINAL ARTICLE

Impact of drilling mud on chemistry and microbiology of an Upper Triassic groundwater after drilling and testing an exploration well for aquifer thermal energy storage in Berlin (Germany)

Simona Regenspurg[1] · Mashal Alawi[1] · Guido Blöcher[1] · Maria Börger[1] · Stefan Kranz[1] · Ben Norden[1] · Ali Saadat[1] · Traugott Scheytt[2] · Lioba Virchow[2] · Andrea Vieth-Hillebrand[1]

Received: 9 March 2018 / Accepted: 28 June 2018 / Published online: 6 July 2018

Abstract

After completion of an exploration well, sandstones of the Exter Formation were hydraulically tested to determine the hydraulic properties and to evaluate chemical and microbial processes caused by drilling and water production. The aim was to determine the suitability of the formation as a reservoir for aquifer thermal energy storage. The tests revealed a hydraulic conductivity of 1–2 E-5 m/s of the reservoir, resulting in a productivity index of 0.6–1 m^3/h/bar. A hydraulic connection of the Exter Formation to the overlaying, artesian "Rupelbasissand" cannot be excluded. Water samples were collected for chemical and microbiological analyses. The water was similarly composed as sea water with a maximum salinity of 24.9 g/L, dominated by NaCl (15.6 g/L Cl and 7.8 g/L Na). Until the end of the tests, the water was affected by drilling mud as indicated by the high pH (8.9) and high bicarbonate concentration (359 mg/L) that both resulted from the impact of sodium carbonate (Na_2CO_3) additives. The high amount of dissolved organic matter (> 58 mg/L) and its molecular-weight distribution pattern indicated that residues of cellulose, an ingredient of the drilling mud, were still present at the end of the tests. Clear evidence of this contamination gave the measured uranine that was added as a tracer into the drilling mud. During fluid production, the microbial community structure and abundance changed and correlated with the content of drilling mud. Eight taxa of sulfate-reducing bacteria, key organisms in processes like bio-corrosion and bio-clogging, were identified. It can be assumed that their activity will be affected during usage of the reservoir.

Keywords ATES · Aquifer thermal energy storage · Drilling mud · Geochemistry · Microbiology · Hydraulic testing · Sulfate reduction

Introduction

The development and installation of aquifer thermal energy storages (ATES) holds great potential for storing heat in the underground (Lee 2013). An ATES system typically consists of two wells, a "hot" and a "cold" one. To store heat, a geofluid is pumped out of a (cold) well, heated up, and then re-injected to the aquifer via a second (hot) well. For utilizing the stored heat, the flow direction will be reversed. The feasibility of energy systems with aquifers was shown in various projects (e.g., Paksoy et al. 2009). However, although ATES systems are already installed in some locations in Germany (Berlin, Rostock, and Neubrandenburg) and are successfully running since several years (Sanner et al. 2005; Kabus et al. 2009; Bauer et al. 2010), operators still hesitate to drill more ATES wells. The main reasons for this situation seem to be linked to geological risks (finding suitable geological storage formations) or to concerns about a safe operation over time, i.e., the fear of potentially damaging the reservoir during operation of the wells by uncontrolled chemical reactions resulting in mineral precipitation and thus reducing the permeability of the reservoir rock. Those damages can be caused, for example,

Electronic supplementary material The online version of this article (https://doi.org/10.1007/s12665-018-7696-8) contains supplementary material, which is available to authorized users.

✉ Simona Regenspurg
regens@gfz-potsdam.de

[1] Helmholtz Centre Potsdam, GFZ German Research Centre for Geosciences, Telegrafenberg, 14473 Potsdam, Germany

[2] Institut für Angewandte Geowissenschaften, Technische Universität Berlin, Straße des 17. Juni 135, 10623 Berlin, Germany

by air oxygen entering into an anoxic reservoir. Thereupon, dissolved ions such as iron (Fe^{2+}) and manganese (Mn^{2+}) can oxidize and precipitate as oxide and hydroxides. Moreover, the dissolved oxygen strongly enhances corrosion of steel casing (Müller et al. 2017; Mundhenk et al. 2013). Especially, the increase of temperature in the aquifer during heat storage can result in increased fluid–rock interaction and microbial activity (Feldbusch et al. 2013; Schneider et al. 2014; Stober and Bucher 2014; Stober et al. 2014). The importance and effects of microbially mediated processes on the reliability of engineered underground installations were discussed in several studies (Beech and Sunner 2004; Little and Lee 2007; Javerhadashti 2008). For example, sulfate-reducing bacteria, frequently found in deep aquifers, are known to be involved in bio-corrosion and its resulting precipitation products such as iron sulfides (Alawi et al. 2011; Lerm et al. 2011). It was found that organic-rich drilling mud induces microbial precipitation of amorphous FeS (Pellizzari et al. 2017) and that certain microbial taxa could be indicative for drilling mud-contaminated groundwater (Struchtemeyer et al. 2011).

Both, biotic and abiotic reactions, can favor precipitation of minerals in the geothermal well, above ground facilities, or in the pore space of the reservoir contributing to a long-term reduction of the permeability/hydraulic conductivity. This affects the reliability and operating life of an ATES system, leading in the worst case to failure of the entire project (Müller and Regenspurg 2014; Regenspurg et al. 2016). The assessment of changes in pore space and the knowledge about the associated processes are, therefore, fundamental for a long-term and safe operation.

The combination of extensive hydrogeological exploration and an experimental hydraulic–chemical and microbial testing program can contribute to understanding such scenarios and to take eventually measure for ensuring an optimal performance of the storage facility. For this reason, an ATES exploration well (GtBChb 1/2015) was drilled in 2016 within the centre of the city of Berlin (Germany). The purpose of drilling the well was to investigate and optimize ATES systems in an urbanized area and to understand the reactions occurring during each step within the development of an ATES site.

This present study aims at characterizing fluid properties and processes occurring at a very early stage right after drilling to obtain information about (a) the aquifer properties and origin of the water; (b) the impact of drilling operations on fluid properties; (c) the chemical and biological processes of relevance when operating an ATES system at the site.

Site description, drilling, and well completion

The city of Berlin is located in the North German Basin, which is a large sedimentary structure in western and central Europe stretching geographically from England in the west to the eastern border of Poland. The North German Basin represents one of those regions with a significant geothermal potential in Germany—both for the use of deep geothermal energy and for thermal aquifer storage. The drilling of the ATES exploration well Gt BChb 1/2015 started in February 2016. The drilling site is located above the flank of a deeper Permian salt structure, rising upwards from east to west. The rise of the Zechstein salt (in Triassic and mainly Jurassic times) resulted in a deformation and dipping of the overlying deposits. Prior to the drilling, it was an open question, if Jurassic sediments may still be present at depth or if they were (due to the salt uplift) already eroded. The first formations overall not influenced by the salt tectonic were the Tertiary and Quaternary units. The exploration well was vertically drilled down to a final depth of 560 m. Up to this depth, only one sequence proved to be appropriate for the use as an ATES reservoir. As a prerequisite, the reservoir unit should have a sufficiently high permeability and should not to be used for drinking water purposes. Therefore, to avoid any utilization conflicts, only formations below the Rupelian clay ("Rupelton", Fig. 1) were considered. The Rupelton acts as a regional aquitard and separates the deeper saline groundwater from Tertiary and Quaternary fresh water above, which are used for drinking water supply. Remarkably, no Jurassic deposits were encountered during drilling. The stratigraphic classification of the various formations was performed on lithological correlation and on first paleontological and

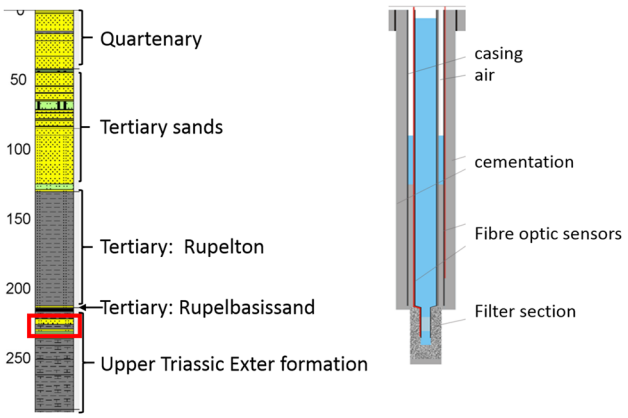

Fig. 1 Left: stratigraphic overview of the exploration well Gt BChb 1/2015 with different geological formations encountered. The red square indicates the location of the filtered section at a depth of 220–230 m. Right: completion scheme of the well

palynological analysis of drill cuttings (Saadat et al. 2016). Based on the drilling results, the sandy, upper part of the Upper Triassic Exter Formation was selected for testing as ATES target formation (Fig. 1).

Well logging (gamma density and neutron logs) indicated porosities of this interval of around 30%. The retrieved respective drill cuttings were characterized as a fine-grained, poorly cemented but well-sorted quartz sandstone with variable organic and calcareous contents interbedded with more silty layers. The total thickness of the sandy horizon amounts to about 4 m between a depth of 221 and 226 m below ground surface.

Right before drilling through the Exter Formation, a thin (only some decimeters thick) sand and lignite containing layer, interpreted as a reworked horizon at the base of the Tertiary Rupelton (the "Rupelbasissand", Fig. 1), was drilled between 212.5 and 213.8 m causing an artesian discharge of approximately 1 m^3/h. After increasing the drilling mud density from 1020 to 1050 kg/m^3, the water table fell again. Due to the proximity between the sandstones of the Exter Formation and the Rupelbasissand, a hydraulic connection between the two cannot be excluded and will be further discussed in this paper. Moreover, as the Rupelbasissand represents the first horizon not influenced by the deeper salt tectonics, it may connect different deeper aquifer levels which cut out at the base of Tertiary.

After the final depth was reached, the wellbore was back-filled with concrete to 259 m below ground level, and the reservoir section of the Exter Formation was filtered between 220 and 230 m. A stainless steel winding wire filter (DN 80 VA WSt 1.4571; 0.5 mm slot width) was installed behind and a 5 m-long sump pipe below the filter section. Filter sand (0.7–1.2 mm) was piled up in the annulus from 259 to 212 m below surface. Above the filter sand, the hole was sealed with a cement–clay mixture ("Brutoplast") and cemented up to the drill cell in the annulus. After wellbore completion, the well was prepared for testing.

Composition of the drilling mud

The main purpose of drilling mud is for cooling the drill bit, transporting the drilled cuttings to the surface, and stabilizing the borehole. The drilling mud often creates a filter cake around the drilled hole that prevents, on one hand, the drilling fluid to enter a permeable formation and, on the other hand, the formation fluid to flow into the well. Various additives were used at the site and mixed with (local tap) water to assemble the drilling mud and define its properties. Fine-grained calcium carbonate ("chalk"; $CaCO_3$) was added to increase the fluid mud density. Bentonite was added for ensuring well stability and creating the filter cake. The synthetic polymer carboxymethyl cellulose (CMC, "viscopol") enhances this effect and prevents the swelling of clays in the formation by increasing the water-binding capacity (DVGW 1998). Sodium carbonate (Na_2CO_3) was added to raise the pH and soften the water to allow optimal swelling of the bentonites. The high pH value also prevents biological degradation of CMC as well as the flocculation of both the CMC and bentonite during drilling of the cement. In addition, the drilling fluid was labeled with sodium fluorescein (uranine) to determine the amount of formation water that could have been affected by the drilling mud after all (Wiese et al. 2013; McCaughey et al. 2016). Table 1 gives the composition of the drilling mud based on the components which were mixed in 26 m^3 of water on the 23rd of March 2016. At this day, the drilling fluid was completely exchanged and the drilling method switched from air drilling to rotary coring mode at a depth of 214.5 m below ground level, just below the base of the Tertiary. In the course of further drilling, the drilling fluid was repeatedly reassembled with different proportions of additives.

Table 1 Drilling mud additives and properties of the drilling mud as put together on 23rd of March 2016 into 26 m^3 water right before drilling through the Exter Formation at well GtBChb 1/2015

Name	Formula/content	Amount (g/L)
Na-bentonite (mainly montmorillonite)	$Al_{1.67}Mg_{0.33}[(OH)_2Si_4O_{10}]*Na_{0.33}(H_2O)_4$	13.46
Viscopol	Na-carboxymethyl cellulose	6.7
Calcium carbonate ("chalk")	$CaCO_3$	21.15
Sodium carbonate ("soda")	Na_2CO_3	0.96
Uranine	$C_{20}H_{10}Na_2O_5$	0.018
Parameter	**Value**	
pH value	10	
Density	1.05 g/cm^3	

Methods

Hydraulic characterization

The hydrogeological investigations included: (a) for the Rupelbasissand, an estimation of the well productivity based on the artesian discharge; for the Exter sandstone (b), a grain-size analysis of drill cuttings. A hydraulic test program of the reservoir (c) included a lift test (c1), a step rate test (c2), and a production test (c3). These five tests and their evaluation will be briefly summarized.

(a) Artesian discharge

During drilling through the Rupelbasissand (drilling mud density: 1020 kg/m^3), an artesian discharge of approximately $V' = 1$ m^3/h was observed and finally stopped by increasing the density to 1050 kg/m^3. Considering a well length of 214.5 m, the density difference of $\Delta\rho = 30$ kg/m^3 corresponds to a pressure difference of $\Delta p = 0.63$ bar, which gives a productivity index (PI) of:

$$\mathrm{PI} = \frac{V'}{\Delta p}.$$

In addition, the PI was calculated from the hydrostatic water table that was measured by tubing extension above ground (= 1.51 m). After the density increases, the water table fell down to 3.5 m below ground. The drawdown of 5 m corresponds to a pressure difference $\Delta p = 0.51$ bar.

(b) Grain-size analysis

To determine the grain-size distribution of a wet drill cutting sample, 145.3 g (222–224 m depth) was added with 500 mL water for some minutes into an ultrasonic bath and afterwards into an overhead shaker for 2 h. After sieving, the fraction < 125 µm was measured in suspension by a laser particle analyzer (Mastersizer 2000, Malvern) computing automatically the volume percentages for 100 arbitrary grain-size classes. After drying (100 °C), the masses of both fractions were weighed and the sample was sieved (63, 125, 250, 500, and 1000 µm; Fig. 2 left). The masses were calculated from the volume fraction multiplied with the total dry mass of the laser particle analysis. The distribution of the mass fraction indicates one main fraction between 1 and 10 µm and one between 20 and 100 µm. The fraction between 1 and 10 µm corresponds most likely predominantly to bentonite that was added to the drilling mud (Table 1). Under the assumption that this fraction is not part of the drilled rock, a more likely grain-size distribution of the reservoir rock was determined after subtracting this bentonite fraction from the total (Fig. 2 right). The hydraulic conductivity (K) was calculated according to Beyer (1964) and Seelheim (1880) with $d10 = 28.8$ µm, $d50 = 56.4$ µm, and $d60 = 63.7$ µm. Since the coefficient of uniformity $U = d60/d10$ is 2.2, the equations are valid:

Beyer (1964):

$$K\left[\frac{m}{s}\right] = 0.0116 \times d10^2.$$

Seelheim (1880);

$$K\left[\frac{m}{s}\right] = 0.00357 \times d50^2.$$

The hydraulic transmissibility T was calculated assuming a thickness (m) of the Exter sands of 4 m:

$$T = K \times m.$$

(c) Hydraulic tests: lift test, step rate test, and production test

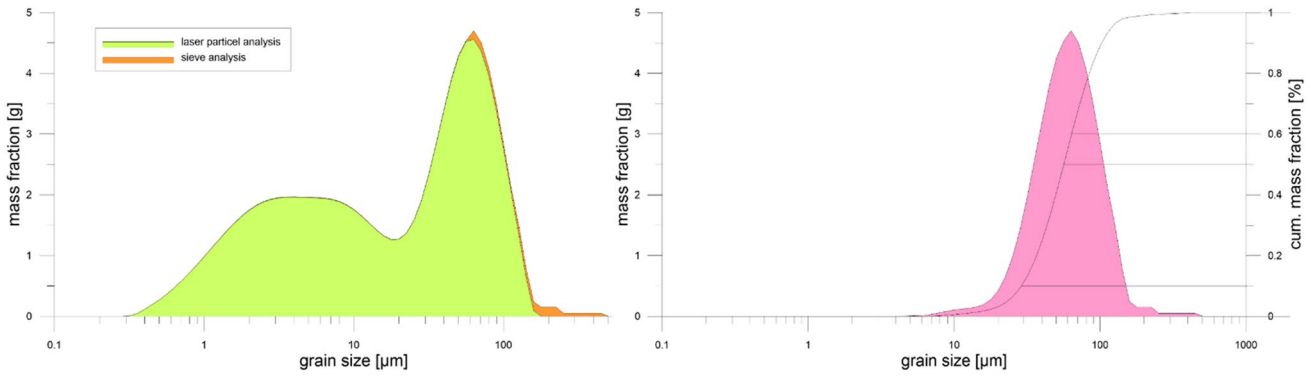

Fig. 2 Left: mass fraction of 100 grain-size classes determined by laser particle and sieve analysis. Right: grain-size distribution and cumulative mass fraction without the bentonite fraction of the drilling mud

Assuming a homogenous and isotropic aquifer, the productivity of the wellbore at constant flow rate was calculated by the non-equilibrium equation (Theis 1935):

$$\frac{V'}{s} = \frac{4 \times \pi \times T}{2.3 \times \lg\left(\frac{2.25 \times T \times t}{r_w^2 \times S}\right)},$$

where V'—flowrate in m^3/s (measured), s—draw down in m (measured), T—hydraulic transmissibility in m^2/s (to be determined), S—storage, dimensionless (to be determined), r_w—well radius in m, $r_w = 0.04$ m, and t—pumping time in s (measured)

(c1) Lift test

An airlift was carried out in the well on the 12th of July 2016 after installing a test string in 75 m depth. Through the bottom end of the string, air was released to the water column, which reduced the density of the water column (1019 kg/m^3) and thereby the hydrostatic pressure. A density of the air/water mixture of 0.5×1019 kg/$m^3 = 509.5$ kg/m^3 was assumed corresponding to a decrease of the hydrostatic pressure of $dp = d\rho \times g \times z = 509.5 \times 9.81 \times 75 = 3.75$ bar. During the lift test, the water table in the water collecting container (base area: 15 m^2; with 1 cm water-level change corresponds to 150 L) was monitored. The change of the water table with the corresponding volume (6.7 m^3) and flow rate (2.87 m^3/h) gives the PI.

(c2) Step rate test

After installing a submersible pump at 92 m and a pressure probe at 110 m depth, a production step rate test was performed on the 14th of July 2016. Consecutively, water at a rate of 1.2, 2, 3, and 5 m^3/h was produced with each step lasting for about 2 h (20.07 m^3 water in total). From the shut-in data, the pressure build-up was calculated which gives the transmissivity (Birsoy and Summers 1980). This analysis is valid for both, unconfined and confined aquifers, and similar to well test analysis with constant flow rate. The shut-in was analyzed using the pressure transient analysis software Saphir NL.

(c3) Production test

Subsequently to the step rate test and after 1 h production stop, water was produced with a flow rate between 5 and 6 m^3/h for another 4 h producing altogether another 20.85 m^3. The corresponding pressure drawdown was about 7.5 bar. This test was also analyzed by Saphir NL.

Chemical monitoring

Altogether, 27 groundwater samples were taken during both, the step rate and the production test. In the following, the given volumes of the produced fluids always refer to the extraction volume starting with the step rate (ignoring the lift) test. Sampling took place immediately after the water reached the surface and before it was flushed into the disposal container. For this purpose, a bypass was installed directly behind a water meter in the delivery hose, where the groundwater was sampled. At this location, also a flow-through cell was installed that contained sensors to monitor physicochemical parameters continuously throughout the pumping tests. The electrodes to measure pH value, electrical conductivity, oxygen, ORP, and temperature were calibrated at the same day and logged automatically at a rate of 5 min.

Samples were immediately analyzed in field for bicarbonate (HCO_3^-) by the methyl orange-titration method. Due to the very high fraction of fine particles in the produced water, a direct filtration was not possible and only trichloro-triflouro-ethane (TTE) was added to each one of the two subsamples for conservation (Banzhaf et al. 2013). Samples were stored cool until arrival in the lab and immediately deep-frozen afterwards. Shortly before analysis, they were defrosted and filtered. Samples were analyzed for cations by inductive coupled plasma optical emission spectrometry (ICP-OES Thermo iCAP 6300 DUO) and for anions by ion chromatography (Dionex DX 120). Uranine was measured by a spectral fluorometer QM-4/2005 (Photon Technology International) at 491 nm (Käss 2004). The dissolved organic content (DOC) was determined with a DOC analyzer in six samples. For a detailed characterization of DOC fractions, four samples collected during the tests (samples 3 and 4 at the beginning of the step rate (after 0.9 and 1 m^3) and samples 26 and 27 (after 38 and 41 m^3) at the end of production test) as well as one sample of the original drilling mud were analyzed in replicates by LC–OCD (liquid chromatography–organic carbon detector). Duplicates existed from each sample (treated with TTE, not treated with TTE) to investigate if the potential presence of bacteria might change the type of DOC fraction after sampling and during storage. The analysis was performed by size-exclusion chromatography (SEC) with subsequent ultraviolet (UV; = 254 nm) and infrared (IR) detection by LC-OCD (DOC-Labor, Germany; Huber et al. 2011). Phosphate buffer (pH 6.85; 2.5 g KH_2PO_4, 1.5 g Na_2HPO_4) served as mobile phase with a flow of 1.1 mL/min. The sample passed a 0.45 mm membrane syringe filter before entering the chromatographic column (250 mm x 20 mm, TSK HW 50S, 3000 theoretical plates, Toso, Japan). After chromatographic separation, the organic fractions were

characterized by UV detection. The DOC fractions were quantified by IR detection of released CO_2 after UV photo-oxidation (185 nm) in a Gräntzel thin-film reactor. By LC-OCD, the dissolved organic matter can be separated into five different fractions referred to as Biopolymers/Macro-1 (> 10,000 Da), Humic Substances/Macro-2 (~ 1000 Da), Building Blocks/Macro-3 (350–500 Da), LMW Acids/Acids (< 350 Da), and LMW Neutrals/Neutrals (< 350 Da; Zhu et al. 2015). External quantification was done using aqueous solutions of potassium hydrogen phthalate in different concentrations (0.1–5 mgC/L). In the same four samples, the amount of organic acids was analyzed by ion chromatography with conductivity detection (ICS 3000, Dionex Corp.). First, the anions were chromatographically separated by the analytical column AS 11 HC (Dionex Corp.) at 35 °C. The sample was eluted by KOH solution with a flow of 0.38 mL/min and varying concentrations over time. The initial KOH concentration (1.4 mM) was maintained for 6 min. After 12 min, 10 mM KOH solution was reached, after 22 min, 15 mM, and after 32 min analysis time, 60 mM KOH concentration was reached, followed by a rapid decrease to 1.4 mM after 33.1 min. This initial level of 1.4 mM was kept for additional 17 min to equilibrate the system. Organic acid standards containing all of the investigated compounds (formiate, acetate, propionate, butyrate, valerate, and oxalate) were analyzed in different concentrations before sample measurement. The standard deviation of sample and standard quantification was below 10%.

Mineral saturation indices were determined by the code PhreeqC vs. 3.3.7.11094 with the llnl database (Parkhurst and Appelo 1999).

Microbial characterization

Sampling and DNA extraction

Four water samples were taken aseptically in sterile 1 L flasks during the step rate and beginning of the production test for microbial analysis after extracting water volumes of 1.46, 4.78, 13.38, and 25.9 m^3. They were filtered (0.2 µm filter screen) within a day and stored at − 20 °C before DNA extraction. Extraction of DNA was performed using the FastDNA spin kit for soil (MP Biomedicals) following the manufacturer's instructions. RNAse-free water was used as a negative control. All sample handling took place in sterile environment. Extracted nucleic acids were quantified with a Qubit+ Fluorometer 2.0. The quality of DNA preparations was checked with the spectrophotometer Nanophotometer® P330. These DNA preparations were used for quantification by quantitative polymerase chain reaction (qPCR) and Illumina MiSeq sequencing.

Quantification of bacterial 16S rRNA genes and functional genes

The total bacterial abundances and the functional genes of sulfate-reducing bacteria as well as of methanogenic archaea were quantified by qPCR as described previously (Krauze et al. 2017). All qPCR essays were performed in triplicates on a CFX96 real-time thermal cycler (Bio-Rad Laboratories Inc., USA). The reactions contained 12.5 µL iTaq™ Universal SYBR® Green Supermix (ThermoFisher Scientific Inc., USA), 8.5–10.5 µl PCR water, the forward and reverse primer (20 µM), and 1–3 µL template DNA. Different dilution factors were tested for each DNA preparation. Bacterial 16S rRNA genes were quantified using the primers 331F (5′-TCCTACGGGAGGCAG-CAGT-3′) and 797R (5′-GGACTACCAGGGTATCTAATCCTGTT-3′) (Nadkarni et al. 2002). After an initial denaturing step of 5 min at 98 °C, 40 cycles of 5 s at 98 °C, 20 s at 57 °C and 60 s at 72 °C plus the plate read were performed. The quantification of sulfate-reducing bacteria was performed using the primers dsr2060F (5′-CAACATCGTYCAYACCCAGGG-3′) (Geets et al. 2006) and dsr4R (5′-GTGTAGCAGTTACCGCA-3′) (Wagner et al. 1998). The following cycling program was used: initial denaturing step of 10 min at 95 °C, followed by 40 cycles of 30 s at 95 °C, 60 s at 60 °C, 60 s at 72 °C, and 3 s at 80 °C plus the plate read. For quantification of methanogenic archaea, the primers mlas-F (5′-GGTGGTGTMGGDTTCACMCARTA-3′) and mcrA-R (5′-CGTTCATBGCGTAGTTVGGRTAGT-3′) were used (Steinberg and Regan 2009). After the initial denaturing step for 3 min at 95 °C, 40 cycles of 5 s at 95 °C, 20 s at 58.5 °C, 30 s at 72 °C, and 3 s at 80 °C plus the plate read were performed. Melting curves were recorded at 60–95 °C with 0.5 °C steps per plate read. The CFX Manager™ Software (Bio-Rad Laboratories Inc., USA) was used to analyze the retrieved data.

Illumina MiSeq sequencing

Preparation of the PCR products for Illumina MiSeq sequencing of the 16S rRNA genes was performed as described before (Krauze et al. 2017). Unique combinations of tagged 515F (5′-GTGCCAGCMGCCGCGGTAA-3′) and 806R (5′-GGACTACHVGGGTWTCTAAT-3′) (Caporaso et al. 2011) primers were assigned to each DNA preparation. Technical triplicates (three independent PCR products) were produced for each biological sample to reduce sequencing variability. Each single technical replicate was tagged with an individual barcode sequence. The PCR was performed on a T100™ Thermal Cycler (Bio-Rad Laboratories Inc., USA) in 25 µL reactions, containing 12.5 µL iTaq™ Universal SYBR® Green Supermix (ThermoFisher Scientific Inc., USA), 8.75 µL PCR water, each 0.625 µL of forward and reverse primer (20 µM), and 2.5 µl genomic DNA. The

following PCR parameters were applied: initial denaturing step for 3 min at 95 °C followed by 10 cycles of 1 min at 94 °C, 1 min at 53 °C (−0.2°C/cycle), and 1 min at 72 °C, followed by 20 cycles of 1 min at 94 °C, 1 min at 50 °C, and 1 min at 72 °C, followed by a final extension step for 10 min at 72 °C. Samples were pooled by adding an equal amount of DNA (60 ng DNA per sample). The PCR product pool was purified with the Agencourt® AMPure® XP- Kit (Beckman Coulter Life Sciences). Illumina MiSeq sequencing (paired-end 2 × 300 bp) was performed by EuroFins Scientific SE, Luxembourg.

Bioinformatics and statistical analysis

Sequence reads were demultiplexed using CutAdapt (options: e0.1; trim-n; Martin 2011). The read pairs were merged using PEAR (options: Q25; p10-4; o20; Zhang et al. 2014). QIIME (version 1.9.1; Caporaso et al. 2010) was employed for further data processing. USEARCH (Edgar 2010) was used to detect and remove chimeric sequences from the data set. The SILVA database (version 128; Quast et al. 2013) was used for open-reference operational taxonomic unit (OTU) clustering (97% sequence similarity) and taxonomic assignments. Singletons and OTUs assigned to chloroplasts were removed before further processing. The PAST3 software was used for multivariate statistics (Hammer et al. 2001). For alpha diversity analyses, the data were rarefied to 32,000 reads per sample. Alpha diversity was estimated using Shannon's H index (diversity) and Shannon's equitability E_H index (evenness). Sequencing data were submitted to the European Nucleotide Archive (http://www.ebi.ac.uk/ena) under accession number PRJEB24963.

Results

Hydraulic properties of the reservoir

The hydraulic properties of the Rupelbasissand were determined by evaluation of the artesian discharge and for the Exter Formation by grain-size analysis and wellbore tests (lift test, step rate test, and production test). The estimated productivity of the Rupelbasissand is nearly twice as high as the measured productivity of the Exter Formation (Table 2). The hydraulic conductivity K of the Exter Formation sand is between 3.8×10^{-6} and 2.5×10^{-5} m/s, which corresponds to a PI of 0.63–1.0 m^3/(h bar; Table 2).

Hydrochemistry of water samples

In situ fluid monitoring revealed that, during the production tests, the specific electrical conductivity (EC) varied between 27 and 42.5 mS/cm (Fig. 3a). After strong initial fluctuations, the EC stabilized between 40 and 41 mS/cm and decreased at the end of the step rate test down to 38.5 mS/cm within 15 min but increased again after a later re-start of the pump (begin of the production tests) to 40.2–41.3 mS/cm (Fig. 3a). Correspondingly, the content of total dissolved solid (TDS) varied between 23.6 and 24.9 g/L. The temperature of the produced water increased first from 15.5 to 17.6 °C and decreased after production of 13 m^3 down to 17.2 °C (Fig. 3a). The fluid was permanently anoxic (dissolved oxygen < 0.1 mg/L), the redox potential varied between −172 and −120 mV, and the pH value increased initially from 8.7 to 10.2 and decreased afterwards to 8.9 (Fig. 3a).

Chloride (Cl^-) and sodium (Na^+) are the dominant ions in the water samples. While the Cl^- concentration varied between 14.4 and 15.6 g/L, Na^+ constantly decreased from 8.1 to 7.8 g/L (Fig. 3b). Similarly, a decrease of the sulfate (SO_4^{2-}) concentration from 715 to 662 mg/L was observed, while calcium (Ca^{2+}) showed a slight upward trend from 144 to 203 mg/L (Fig. 3b). The magnesium (Mg^{2+}) and potassium (K^+) concentration were relatively stable from 174 to 187 mg/L and from 55 to 62 mg/L, respectively. Bicarbonate (HCO_3^-) was between 426 and 201 mg/L, with a sudden decrease followed by an increase in concentration in the fourth stage of the step rate test. Similarly, carbonate (CO_3^{2-}) decreased from 187 to 35 mg/L (Fig. 3b). The uranine concentration decreased from 0.101 mg/L in the beginning of the test to 0.044 mg/L in the end (Fig. 3c). After producing 2–3 m^3 (about one borehole volume), a concentration

Table 2 Hydraulic properties of the Rupelbasissand and of the Exter Formation sandstone determined by wellbore tests and grain-size analysis

Test	Formation	k_f (m/s)	Transmissivity (m^2/s)	PI (m^3/h/bar)
Artesian discharge	Rupelbasissand	–	–	1.58–1.96
Grain-size analysis	Exter	9.6e−06 to 1.1e−05	4.0e−05	1.00
Lift test	Exter (+Rupelbasissand?)	–	–	0.76
Step rate production		2.1e−05^S	8.5e−05^S	0.63
Step rate shut-in		3.8e−06 (1.3e−05^S)	1.5e−05 (5.3e-05^S)	–
Production test		2.5e−05^S	9.8e−05^S	0.7

The superscript S denotes values obtained by Saphir NL, which is the industry standard for pressure transient analysis software

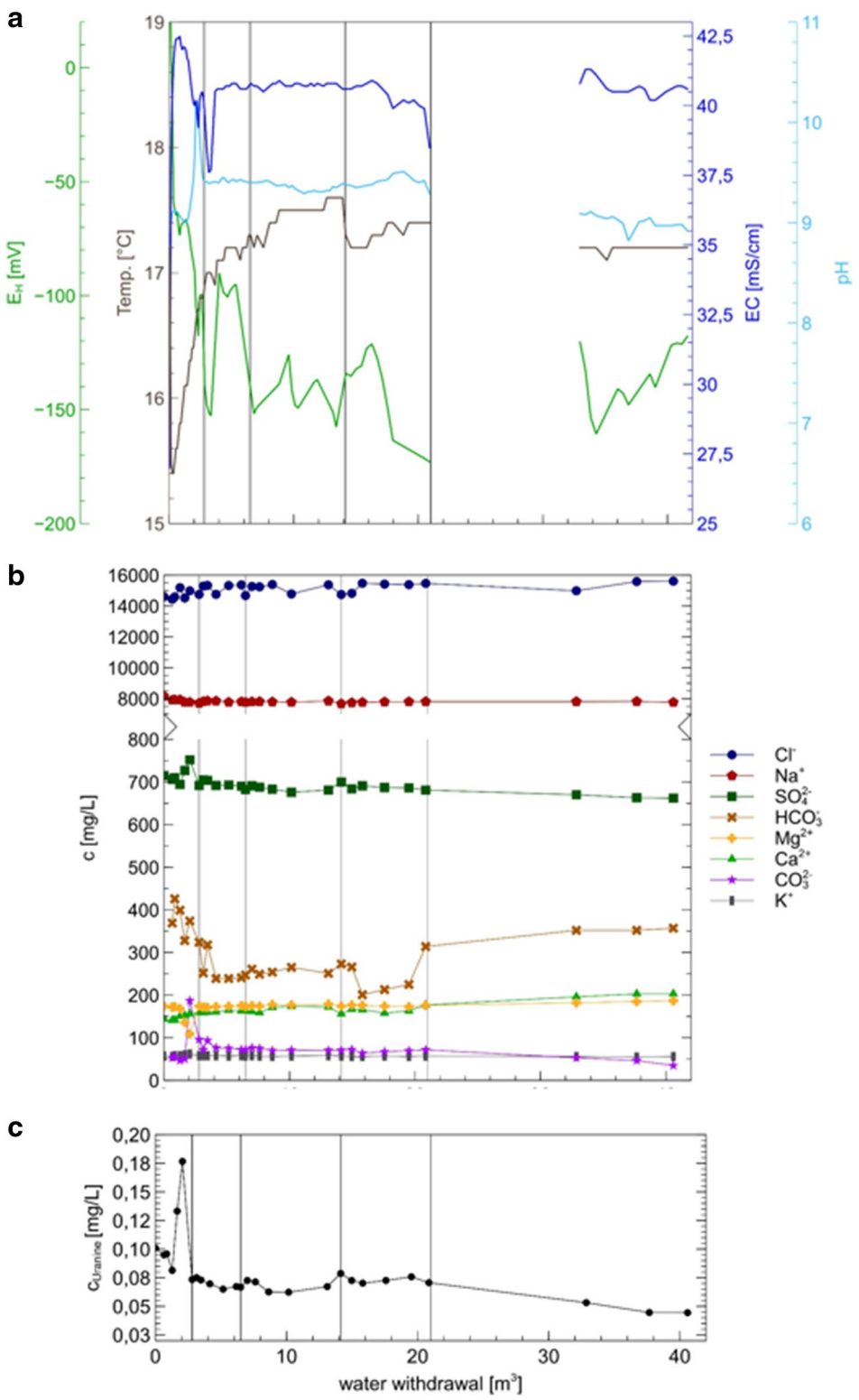

Fig. 3 Measurements during the step rate and production test in dependence on produced fluid. **a** Physicochemical parameter measured in situ; **b** concentration of ions measured in collected samples; **c** concentration of uranine tracer measured in collected samples

maximum of CO_3^{2-}, HCO_3^-, SO_4^{2-}, and uranine as well as a minimum of Mg^{2+} were observed (Fig. 3b, c).

Concentrations of strontium (Sr^{2+}: 8–10 mg/L), lithium (Li^+: 0.62–0.56 mg/L), and manganese (Mn^{2+}: 0–0.07 mg/L) were low, and no significant changes in concentration were observed over time. Copper (Cu^+), iron ($Fe^{2+/3+}$), lead (Pb^{2+}), bromide (Br^-), fluoride (F^-), phosphate (PO_4^{3-}), and nitrite (NO_2^-) were below the detection limit of the

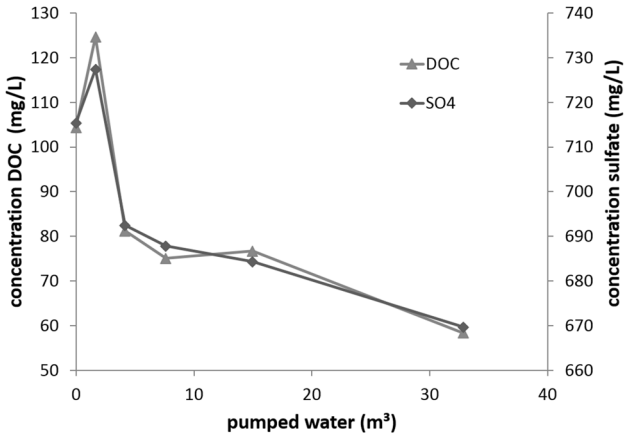

Fig. 4 Correlation of DOC and sulfate in the samples collected during the step rate and production tests

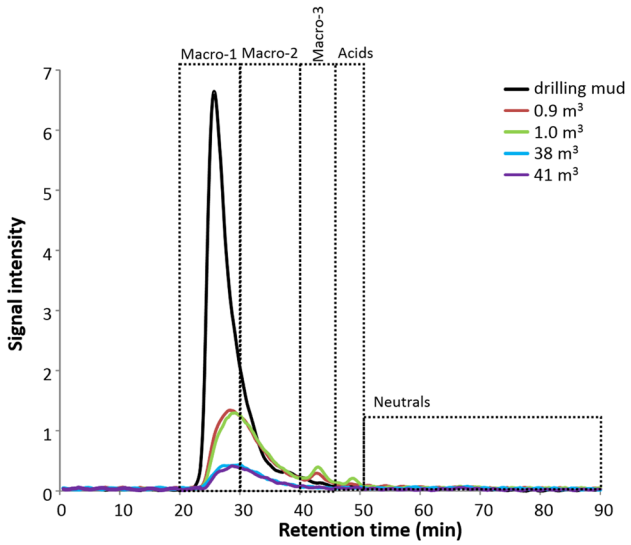

Fig. 5 LC-OCD measurement showing molecular-size distribution of drilling mud and water samples collected during the step rate and production test

used instruments. The DOC concentrations showed a highest value of 125 mg/L in the beginning decreasing linearly towards the end of the pumping tests to 58.3 mg/L. Positive correlations were found between uranine, DOC, and SO_4^{2-} (Fig. 4). Similarly, Na^+, Cl^-, and TDS positively correlated, whereas a negative correlation was observed between Ca^{2+}, Mg^{2+}, and SO_4^{2-}.

Calculation of the saturation index (SI) revealed that the carbonate minerals aragonite, calcite, and magnesite (all between SI = 1.4 and 2.2) as well as dolomite (SI = 4.7–5.7) are the only minerals being supersaturated.

Characterization of dissolved organic matter

The molecular-size distribution of the DOC was characterized both, in the drilling mud and in samples collected at the beginning (sample 3 and 4) as well as at the end (samples 26 and 27) of the fluid production test (Fig. 5). While, in the initial drilling mud, 1194 mg C/L DOC were measured by LC-OCD, this amount decreased to 24.7 mg C/L at the end of the tests corresponding to roughly 2%. The chromatograms clearly show that the drilling mud is dominated by high-molecular-weight compounds, while organic compounds with lower molecular weight only occur in low amounts. In general, this distribution pattern of the drilling mud can also be observed in the samples from the production tests but on a lower intensity level. The peak maximum of this macro-fraction is slightly shifted to higher retention times for the fluid samples in comparison to the drilling mud (Fig. 5). No difference in amount and type of the DOC fractions was identified between TTE treated or non-treated samples. Results of organic acid analysis by IC, measured in the same samples, revealed only formate being present at concentrations slightly above the detection limit (10 mg/L) in one sample collected at the beginning (17.4 mg/L) and in one sample collected at the end of the pumping test (11.6 mg/L). The detection limit for organic acids is relatively high due to strong dilution of the samples that was necessary because of the high chloride concentrations.

Microbial analysis

Microbial abundance

The abundance of bacteria increased in the initial phase of the pump test and decreased towards the end. After extraction of 1.08 m^3 water, 1.3×10^9 gene copies L^{-1} were measured. After the extraction of 25.9 m^3, the gene copy number decreased by one order of magnitude to 2.3×10^8 gene copies L^{-1} (Fig. 6a). Similarly, the number of sulfate-reducing bacteria (*dsrB* gene) decreased towards the end of the production test: After extraction of 1.08 m^3 water, 4.9×10^6 gene copies L^{-1} water were detected, which decreased slightly after 4.7 m^3 (4.1×10^6 copies L^{-1}) and more drastically after 13.38 m^3 to 1.5×10^6 gene copies L^{-1} (Fig. 6a). In contrast to the total cell number and sulfate-reducing bacteria, the abundance of methanogenic microorganisms (*mcrA* gene) increased over time of water production from 1.3×10^3 gene copies L^{-1} to 3.9×10^3 gene copies L^{-1} (Fig. 6).

Diversity and microbial community composition

After read merging, demultiplexing, quality filtering, and deletion of chimeric sequences, 785,366 reads were obtained. The amount of reads per sample ranged from 29,937 to 135,665 with a mean value of 65,447. Rarefaction

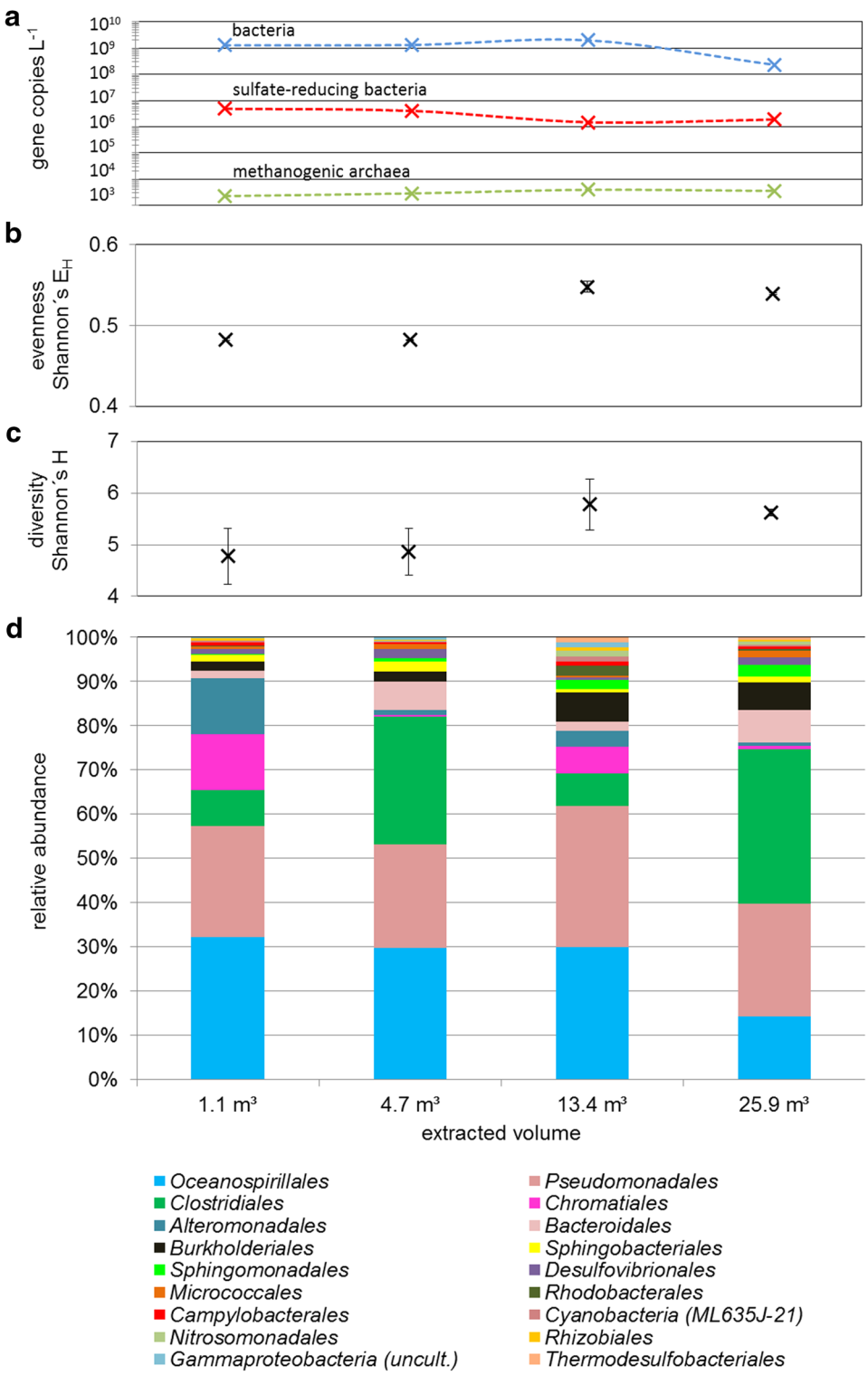

Fig. 6 **a**. Abundance of bacteria (16S rRNA gene), methanogenic archaea (mcrA gene), and sulfate-reducing bacteria (dsrB gene) in samples collected after different extraction volumes of the step rate test. Mean values (triplicates) from qPCR analyses; **b** Shannon's E_H index indicated an increase in species evenness with increased volume of extracted water; **c** Shannon's *H* index indicated an increased microbial diversity with increased volume of extracted water; **d** shifts in the microbial community composition were observed with an increased volume of produced water. Data were obtained by Illumina high-throughput sequencing of 16S rRNA genes. Only taxa (order level) with a relative abundance > 0.4% are shown. All data are mean values of triplicates

analyses showed that no sample exhibited a conspicuous increase of its Shannon's *H* index after including more than 14,008 sequences. All samples have been sufficiently covered by sequencing, since an increasing number of reads per sample do not bias diversity. A total of 5571 OTUs were retrieved after singletons, chloroplast-related OTUs, and OTUs that could not be assigned at the level of domain were removed (supplement S1). After triplicates were merged by mean value, 183 taxa at order level and 557 putative genera were obtained. Applying a 0.4% cutoff, 18 putative taxa at

order level remained (Tab. S2). 77 putative genera (14% of all genera) could no longer be observed at the end of the extraction phase (Tab. S3).

The species evenness (how close in numbers each species is in an environment) increased as indicated by the Shannon's E_H index (Fig. 6b). At the same time, Shannon's H index, which gives an impression of the microbial diversity (number of individuals as well as number of taxa) increased with the volume of extracted water (Fig. 6c). During the course of water extraction, shifts in the microbial community were observed. With increased production volume, the relative abundance (within the whole community) of bacteria of the order *Chromatiales, Alteromonadales*, and *Oceanospirillales* decreased. The relative abundance of SRB of the order *Desulfovibrionales* fluctuated. Bacteria of the order *Thermodesulfobacteriales, Clostridiales*, and *Cytophagales* increased in relative abundance during the course of production (Fig. 6d).

The 30 most abundant putative taxa of samples taken at the end of the water extraction (25.9 m^3) amounted to 88.6% of all reads (Table 3). In total, 3% of all reads of the sample taken at the end of the extraction phase were assigned to SRB. *Desulfomicrobium* (1.3% of total reads from the last sample), *Desulfosporosinus* (0.8%), and *Thermodesulfobacterium* (0.5%) were the most abundant taxa. The relative abundance of SRB increased for six of the eight taxa during the course of fluid extraction. The relative abundance of *Thermodesulfobacterium, Desulfurivibrio*, and *Desulfotomaculum* showed an 8-, 10- and 12-fold increase during the water extraction phase. A small decrease was observed for the genera *Desulfomonile* and *Desulfobacca* (Table 3).

Table 3 30 most abundant taxa in the samples taken at the end of the step rate test (25.9 m^3)

Relative abundance (%)	Putative taxa
23.4	*Bacteria; Firmicutes; Clostridia; Clostridiales; Ruminococcaceae; Ercella*
22.4	*Bacteria; Proteobacteria; Gammaproteobacteria; Pseudomonadales; Pseudomonadaceae; Pseudomonas*
13.2	*Bacteria; Proteobacteria; Gammaproteobacteria; Oceanospirillales; Halomonadaceae; Halomonas*
5.1	*Bacteria; Bacteroidetes; Bacteroidia; Bacteroidales; Prolixibacteraceae; Sunxiuqinia*
5.0	*Bacteria; Firmicutes; Clostridia; Clostridiales; Lachnospiraceae*
1.7	*Bacteria; Proteobacteria; Deltaproteobacteria; Desulfovibrionales; Desulfomicrobiaceae; Desulfomicrobium*
1.6	*Bacteria; Proteobacteria; Betaproteobacteria; Burkholderiales; Comamonadaceae*
1.4	*Bacteria; Firmicutes; Clostridia; Clostridiales; Peptococcaceae; Desulfosporosinus*
1.4	*Bacteria; Proteobacteria; Alphaproteobacteria; Sphingomonadales; Sphingomonadaceae; Sphingomonas*
1.2	*Bacteria; Proteobacteria; Betaproteobacteria; Burkholderiales; Comamonadaceae*
1.0	*Bacteria; Proteobacteria; Betaproteobacteria; Burkholderiales; Burkholderiaceae; Ralstonia*
1.0	*Bacteria; Proteobacteria; Alphaproteobacteria; Sphingomonadales; Sphingomonadaceae; Sphingobium*
0.8	*Bacteria; Firmicutes; Clostridia; Clostridiales; Eubacteriaceae; Alkalibacter*
0.8	*Bacteria; Proteobacteria; Betaproteobacteria; Burkholderiales; Oxalobacteraceae*
0.8	*Bacteria; Bacteroidetes; Bacteroidia; Bacteroidales; Porphyromonadaceae; Macellibacteroides*
0.7	*Bacteria; Proteobacteria; Gammaproteobacteria; Alteromonadales; Idiomarinaceae; Aliidiomarina*
0.7	*Bacteria; Proteobacteria; Gammaproteobacteria; Chromatiales; Chromatiaceae; Rheinheimera*
0.7	*Bacteria; Actinobacteria; Actinobacteria; Micrococcales; Demequinaceae; Demequina*
0.7	*Bacteria; Bacteroidetes; Bacteroidia; Bacteroidales*
0.6	*Bacteria; Firmicutes; Bacilli; Bacillales; Staphylococcaceae; Staphylococcus*
0.6	*Bacteria; Bacteroidetes; Sphingobacteriia; Sphingobacteriales; CMW-169 bacterium*
0.6	*Bacteria; Proteobacteria; Gammaproteobacteria; Pseudomonadales; Moraxellaceae; Moraxella*
0.5	*Bacteria; Thermodesulfobacteria; Thermodesulfobacteria; Thermodesulfobacteriales; Thermodesulfobacteriaceae; Thermodesulfobacterium*
0.5	*Archaea; Altiarchaeales euryarchaeote euryarchaeote euryarchaeote euryarchaeote*
0.5	*Bacteria; Proteobacteria; Betaproteobacteria; Nitrosomonadales; Gallionellaceae; Gallionella*
0.5	*Bacteria; Proteobacteria; Betaproteobacteria; Burkholderiales; Oxalobacteraceae; Undibacterium*
0.4	*Bacteria; Firmicutes; Clostridia; Clostridiales; Family XII; Fusibacter*
0.4	*Bacteria; Proteobacteria; Alphaproteobacteria; Rhodospirillales; Rhodospirillaceae; Skermanella*
0.4	*Bacteria; Actinobacteria; Actinobacteria; Micrococcales; Micrococcaceae; Micrococcus*
0.3	*Bacteria; Cyanobacteria; ML635J-21*
11.4	Other 552 taxa

Discussion

Water origin and mixing with drilling mud

The reservoir quality of the sandstones is known to be strongly facies-dependent (Barth et al. 2013). Sandstones of the Exter Formation have been described as poorly cemented with porosities of 25–30%, permeabilities of 500–1000 mD, and productivities of 5–15 m^3/h/bar (Stober et al. 2014). In this study, the permeability of the Exter Formation as calculated from grain-size analysis of cuttings amounts to 1×10^{-6} to 1×10^{-5} m/s corresponding to 100–1000 mD. The Exter Formation was deposited about 200 Mio years ago at the boundary area of a former delta and its fluids are described as saline (Wolfgramm et al. 2011). Compared to other analyzed reservoir fluids of the Exter Formation in the North German Basin, the samples collected in this study contain lower concentrations of the main elements Na, K, Mg, Ca, and Cl (Fig. 7; Wolfgramm et al. 2011; Wiese et al. 2013). This could either be attributed to slight differences and depths of the Exter Formation (due to different structural settings) or to the dilution of the measured sample with drilling fluid. The latter explanation seems likely, considering that the sandstone of the Exter Formation together with the overlaying Tertiary sands have been an open-well over 3 months being exposed to the drilling fluid before the casing was installed. Furthermore, borehole wall outbreaks caused large contact surfaces between the formation and the drilling fluid in these depths. Unfortunately, there are no records of the amounts of those fluid losses. Due to the long contact time, however, it is very likely that the drilling fluid penetrated the formation in larger quantities. A similar observation was made by Pellizzari et al. (2013) at the Ketzin research well, demonstrating that drilling mud penetrated through micro-fractures into sandstone during drilling. The low Ca and the high HCO_3 content as well as the high pH values of the samples collected here indicate that the reservoir water was still mixed with the lower saline drilling fluid. An even stronger indicator for the presence of the drilling fluid is the tracer uranine: The fluorescence tracer was added to the drilling mud only (Table 1) and does not occur naturally. Since uranine was detected in all collected groundwater samples, it is obvious that they were all still affected by the drilling fluid. The drilling mud components DOC, uranine, Na^+, and HCO_3^- all decreased with increasing amount of produced fluid, indicating that the drilling mud was gradually pumped out of the reservoir, while, at the same time, components of the reservoir water such as Cl^-, Mg^{2+}, and Ca^{2+} increased. Interestingly, sulfate, which was not added to the drilling mud, also decreased over time—an observation that will be further discussed in context with the microbial activities ("Changes in the microbial abundance and community composition").

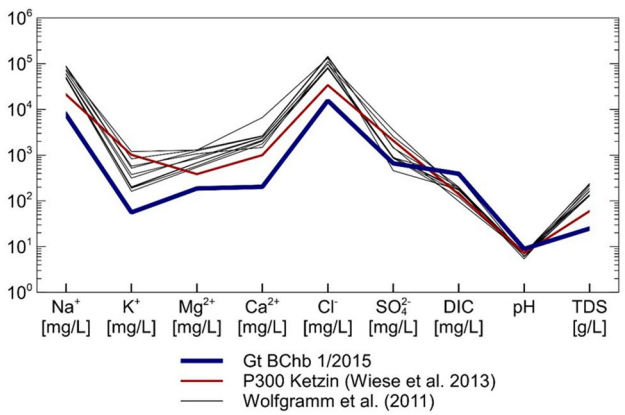

Fig. 7 Schöller diagram with elemental composition of the Exter Formation water in the North German Basin. Blue line: measured values of this study (the last sample collected during the production test); red line: fluid from the Exter Formation of the well Ketzin P300 (Wiese et al. 2013); black lines: data from several wells producing Exter Formation water (Wolfgramm et al. 2011)

Apart from dilution of drilling fluid components in the formation of water, also adsorption and ion exchange need to be considered. It is very likely that cations interact with the negatively charged clay mineral surfaces that were introduced with the drilling fluid (bentonite) enabling an increased cation exchange (Appelo and Postma 2009; Langguth and Voigt 2004) and impedes the determination of fluid mixing ratios. Adsorption and ion exchange also explain why cations such as K^+, Li^+, and $Sr2^+$ showed all relatively constant concentrations, although one would assume them to increase with increasing produced volume, since they are also not ingredients of the drilling mud.

A quantification of the amount of drilling mud within the produced fluid is difficult, because all indicators (uranine-, DOC-, bicarbonate concentration) have different pathways on distributing in the environment: uranine might adsorb to minerals at increased salinity of the water (Magal et al. 2008), the organic compounds could be oxidized by microorganisms to CO_2, and bicarbonate could have precipitated as a carbonate mineral, since calcite, dolomite, and aragonite were all calculated to be oversaturated. Moreover, the amount of bicarbonate and DOC is not known in the pristine formation fluid and, since drilling mud of different composition was added permanently during drilling, the actual volume that entered the formation remains also unknown. However, when assuming that uranine would have behaved conservatively in the reservoir, 0.7% of the originally added amount of drilling mud (Table 1) would still be in the reservoir water in the beginning of the test decreasing to 0.35% towards the end. The characterization of DOC by size-exclusion chromatography (LC-OCD) confirmed that DOC in the groundwater samples is comparable to the DOC

in the drilling fluid. The shift of the peak maximum of the macro-fraction to higher retention times for the water samples in comparison to the drilling mud (Fig. 5) indicates the degradation of the cellulose-containing additives over time.

This study also aimed to determine if the produced fluid is only derived from the Exter Formation or if the Tertiary Rupelbasissand also contributes to the observed hydraulic and chemical properties. This could be of significance, because the PI of the Rupelbasissand is clearly higher as the PI of the Exter Formation (Table 2). Indeed, grain-size analysis of the Exter sands resulted in slightly lower hydraulic conductivities as compared to the hydraulic conductivity obtained from the hydraulic tests (Table 2). This could be explained by a hydraulic connection of the Exter Formation with the Rupelbasissand. Since there is no knowledge on the chemical composition of the undisturbed fluids of neither this aquifer nor of literature data from the Rupelbasissand, a mixing effect based on the current geochemical data was not identified. The measured groundwater composition resembled mainly a slightly diluted Exter Formation fluid as compared to the literature data (Fig. 7). Solely, the relatively higher sulfate concentration (that was not part of the drilling mud) could be an indication for input of a different water type (Fig. 7). On the other hand, sulfate also plays a significant role in microbial reactions as discussed in the following.

Changes in the microbial abundance and community composition

To track changes in the microbial community of groundwater during a hydraulic test, fluid samples were taken after different extraction volumes and analyzed. Complementary to the abiotic tracer uranine, DOC, and bicarbonate, it was evaluated whether the microbial abundance and the community composition might be indicative for the extent of which drilling mud is admixed in produced fluids and influenced the microbiology of the well-near area in the reservoir. In addition, the diversity and abundance of sulfate-reducing bacteria, potentially involved in detrital effects on the reservoir and underground installation, was tracked. Different effects of the organic-rich drilling mud on the microbiology of well fluid and well-near technically influenced reservoir fluid were observed. Especially, the first cubic meters of produced fluid showed high abundances as well as a decreased diversity, characterized by the dominance of a few taxa (Fig. 6d). These effects were still present, albeit to a lesser extent in the further course of extraction.

As indicated by data from geochemical analyses, the high microbial biomass in samples from the beginning of the extraction phase (10^9 gene copies L^{-1}; Fig. 6a) was triggered by a strong admixture with residual drilling mud. The high bacterial abundance could also be indicative for the formation of biofilms during the months of which residual drilling mud remained in the well before casing. Such biofilms were described, for instance, in an aquifer storage in Neubrandenburg (Germany, Lerm et al. 2011). Both effects also explain the decrease of the bacterial abundance (10^8 gene copies L^{-1}) by one order of magnitude with increased production volume (Fig. 6). Similarly, but to a lower degree, the abundance of SRB decreased with the amount of produced fluid. The impact of organic drilling mud components on the SRB community and subsequently detrital effects on the well injectivity was highlighted by Morozova et al. (2010), showing that after clean-up of the wells by a N_2 lift, the total microbial cell number and the number of SRB decreased by at least two orders of magnitude. The authors explained a strongly increased cell number in the well fluid prior to the cleaning with the increased availability of organic substrates provided by drilling mud. Struchtemeyer et al. (2011) analyzed drill fluids from seven wells and concluded that the initial cell counts from water used for the mud are typically low (10^3–10^5 gene copies L^{-1}) but increase (10^6–10^7 gene copies L^{-1}) after addition of organic-rich thickeners such as cellulose. Furthermore, sulfur compounds such as barite and lignosulfonates are potential substrates for microorganisms. A slight increase of the abundance of obligate anaerobic methanogens at the end of the pump test might indicate that the fluid after producing 25.9 m^3 represents, to a higher degree, the microbial composition of the formation fluid. It also has to be considered that, due to an increased microbial degradation of organic substance in the well-near area, the amount of potential substrates for methanogens such as acetate may have triggered their growth.

Parameters that are important for understanding the microbial ecology of a system, namely the microbial diversity (Shannon's H index) and species evenness (Shannon's E_H), clearly indicated a strong influence of drilling mud on the microbial community at the beginning of the pump test. The drilling mud-influenced water provided optimal growth conditions for organoheterotrophic organisms. It is known that, under conditions with high amounts of organic substances (such as from drilling mud), these microorganisms can grow and proliferate. Such artificial systems are generally characterized by a low microbial diversity but high cell numbers. With the increased volume of produced fluid, the microbial diversity and species evenness increased significantly, and more taxa originating from the reservoir were admixed. Conclusively, tracking the alpha diversity indices may provide a further tool for assessing the degree to which well-extracted formation fluids are influenced by technical fluids or whether the reservoir community shifts in a long-term perspective during usage as an ATES.

Microbiological analyses which carried out during the step rate test showed a shift within the microbial community in the pumped fluid (Fig. 6d). Interestingly, there are no taxa that occur solely in the beginning of the step rate

test, indicating that the well fluid was already mixed with formation water. In contrast, 77 genera (14% of all genera) vanished completely at the end of the extraction phase. These taxa are most likely contaminants from the drilling mud-influenced well fluid (supplement S3). They may be useful as indicator organisms for future drillings, assessing the degree of drilling mud admixture in produced water or anthropogenic-induced changes in the reservoir. Some of these taxa were already described in a study at lower sequencing depths by Struchtemeyer et al. (2011). In their study, within the class of *Bacilli*, the families *Bacillaceae, Paenibacillaceae, Planococcaceae*, and *Alicyclobacillaceae* were identified to be typical for drilling mud-influenced fluids. Similarly, within the class of *Clostridia* the genera *Ruminococcus* and *Thermoanaerobacter* and within the *Gammaproteobacteria* the orders *Pseudomonadales* and *Alteromonadales* were linked to drilling mud influences. The results of our study revealed that 37–48% of the total reads can be assigned to these taxa. Even though only the relative abundance of *Alteromonadales* (mainly the genera *Aliidiomarina*) decreased significantly during the pump test from 12.2 to 0.7%, our results led to the conclusion that the autochthonous microbial community of the formation fluids is overlaid from allochthonous "drilling mud bacteria" even at the end of the pump test. Apart from taxa mentioned above, genera such as *Ercella* (23.1% of the reads from the last sample) and *Staphylococcus* (0.7%) indicate anthropogenic contamination by the drilling mud or during sampling procedures.

Microorganisms that are typical for deep aquifers are also observed in all investigated samples. However, due to the high number of allochthonous taxa, typically, their relative abundances are low. In total, 169 taxa (26% of the total reads) increased by at least a factor of two until the end of the production phase. It can be concluded that these taxa represent part of the autochthonous microbial community of the reservoir fluids. For example, a high relative abundance was found for *Sunxiuqinia* (*Cytophagales*; threefold increment, 5% rel. abundance at the end of the pump test) and *Lachnospiraceae* (*Clostridiales*; fourfold increment, 5% rel. abundance). Organoheterotrophic, facultative anaerobic *Sunxiuqinia* were found before in 900 m-deep sub-seafloor sediments (Takai et al. 2013). *Lachnospiraceae* have been isolated from "black smokers" in the deep sea (Schouw et al. 2016). Other putative autochthonous microorganisms like the strictly anaerobic *Ferribacterium* (*Rhodocyclales*) (16-fold increment, 0.23% rel. abundance) or facultative anaerobic *Marinobacter* were less abundant (0.01% rel. abundance). The identified Fe(III)-reducing bacteria of the genera *Ferribacterium* were previously isolated from mining-impacted lake sediments (Cummings et al. 1999). Although the fluids of the Exter Formation could be (if not mixed with younger fluids) up to 200 Mio years old, it has been recently shown that microorganisms found in such old sedimentary basins are alive and can be cultivated (Filippidou et al. 2016).

The observed ratio between dissolved organic carbon (DOC) and sulfate (Fig. 4) can be an indicator for microbially mediated processes, although a dilution effect of the drilling mud has to be considered. Over the course of fluid production, both DOC and the sulfate concentration decreased with a correlation factor $R = 0.94$; Fig. 4. A highly diverse consortium of sulfate-reducing bacteria (eight taxa) could have reduced the amount of sulfate to sulfide, while simultaneously oxidizing organic compounds (the cellulose viscopol; $C_{12}H_2OO_{10}$) according to the following equation:

$$C_{12}H_2OO_{10} + 6SO_4^{2-} + 12\ Na^+ \rightarrow 12\ CO_2 + 6\ S^{2-} + 10H_2O + 12\ Na^+.$$

Since the Fe concentration during the production test decreased simultaneously from 0.03 mg/L to below detection limit, a precipitation of iron sulfides is possible. Assuming sulfate origins only from the reservoir, an increase for about 0.5 mM would be expected. Since, however, sulfate decreased for about 0.5 mM, roughly 1 mM sulfate (96 mg) in total "disappeared". If this amount corresponds to 1/6 mol cellulose (with $M = 324$ g/mol), this would correspond to a total loss of DOC of 23.7 mg/L.

SRB are generally known to inhabit deep aquifers and occur in a high taxonomic diversity (Alawi et al. 2011). The most abundant SRB in the investigated waters, *Desulfomicrobium* (1.3% of total reads) and *Desulfosporosinus* (0.8% of total reads), are known to perform an incomplete oxidation of organic compounds with acetate as end member (Rozanova et al. 1988; Robertson et al. 2001). Therefore, a decrease of DOC can also be coupled to other microbial processes such as acetoclastic methanogenesis, where acetate is converted to CH_4 and CO_2.

Assessment of scaling risks

The precipitation of solid phases ("scaling") within the pores of a reservoir represents one of the largest risks when operating a geothermal or an ATES system (Regenspurg et al. 2015). Depending on the water composition as well as on the temperature and pressure conditions, various types of scales can be expected. Especially, iron oxides, alkaline earth sulfates, and carbonates represent the most common types of scaling known also from geothermal energy systems. While dissolved iron was very low in the investigated samples and represents, therefore, a little risk, the high carbonate concentration (Fig. 3b) resulted in a calculated oversaturation of carbonate minerals (calcite, dolomite, and aragonite) already at ambient temperatures, which would represent an

even larger problem, when the fluid would be heated during hot-water storage due to the retrograde solubility of most carbonates. However, since both sodium carbonate (Na_2CO_3) and calcium carbonate ($CaCO_3$) are additives of the drilling mud (Table 1), the real carbonate concentration in the pristine formation fluid remains still unknown and the estimation of long-term carbonate scaling risk can only be done when the drilling fluid is fully pumped out.

Apart from these abiotic scaling risks, the impact of reactions induced or accelerated by microorganisms has also to be considered. The high abundance of microorganisms could indicate the formation of biofilms (Lerm et al. 2011). Moreover, although sulfate minerals were undersaturated according to PhreeqC calculations, the bacterial reduction of sulfate to sulfides as discussed above could result in the precipitation of sulfides together with metals such as Fe, Cu, and Zn. Although these metals were hardly detected so far in the produced water, bio-corrosion could mobilize Fe from the casing, thus providing the required cations for sulfide mineral precipitation such as pyrite (FeS_2).

Conclusion

Knowledge of the geological nature of the underground and the bio-geochemical reactions therein is indispensable for sustainable and safe use of aquifers. A risk assessment for reservoir-damaging processes potentially occurring in an ATES system is crucial already before utilizing the ATES well and aquifer for heat storage. This study aimed to characterize relevant chemical and microbial reactions that might induce damages to the well or reservoir. Detailed chemical and microbial data were obtained from samples collected during a hydraulic test program right after drilling and completing an ATES exploration well into an Upper Triassic sandstone aquifer in Berlin. A special focus was given on the effect of drilling mud that drained into the reservoir formation during drilling, mixing there with the pristine groundwater.

In all of the water samples taken during the tests, a significant impact of drilling mud was detected that decreased with increasing amount of produced groundwater. The drilling mud affected strongly not only the initial chemical composition but also largely the microbial community in the fluid of the target sandstone. The high-throughput sequencing of the microbial community allowed a detailed view on changes provoked by the drilling mud and the identification of species typical for drilling mud contamination. The high input of organic material contained in the drilling mud strongly changed the microbiology of produced fluids. Both, cell numbers and the microbial community structure, varied over time of the production test, indicating that several microorganism groups are specific to drilling mud and overlaid the natural community found in the formation fluid. Especially, sulfate-reducing bacteria were influenced by the organic-rich drilling mud and were triggered in growth. The observed eight genera of SRB are of special importance for bio-corrosion and microbial-mediated precipitation on a long-term perspective. However, no direct evidence of sulfide formation was detected yet, although the decrease in sulfate concentration could be an indicator for this process. Changes in the chemical properties and temperature regime during the energy storage may trigger such microbial-mediated processes and should, therefore, be included to long-term monitoring programs. In addition to the organic constituents in the drilling mud, also the high amount of carbonate and bicarbonate deriving from added sodium carbonate represents a risk for mineral precipitation. Since many carbonate minerals such as aragonite, calcite, and magnesite were over saturated, it can be assumed that some of them already precipitated in the reservoir. Upon heating the aquifer during hot-water storage, the saturation of these minerals would even increase. Due to these observations and for preventing severe and irreversible damages of the reservoir when drilling a well, it is recommended to either avoid adding organic or carbonate substances into the drilling mud or at least to pump them out of the reservoir as quickly as possible right after drilling to shorten their reaction time with the pristine water. To obtain fluid unaffected by drilling mud, a further pumping test over a longer time is necessary.

Apart of the risk assessment, the study also aimed to obtain information on origin and mixing of the formation water. Since, to the best of our knowledge, no formation water samples or its hydrochemical data of the Rupelbasissand exist, the current study can neither clearly confirm nor refute a hydraulic connection between the hanging artesian Tertiary aquifer and the fluids of the Exter sandstone. However, it must be assumed that (due to the structural dip) the sandstones of the Exter Formation are pinching out at the level of the Rupelbasissand in some distance of the well. Moreover, the PI as determined from the hydraulic tests of the reservoir is between the PI from the Rupelbasissand and that of the Exter cuttings indicating also a mixed fluid.

Acknowledgements The authors gratefully acknowledge Iris Pieper of the "*Geochemisches Gemeinschaftslabor*" at the Technical University of Berlin for inorganic ion analysis and Sarah Zeilfelder for assistance during sampling. Kristin Günther and Georg Schettler from GFZ are acknowledged for the analysis of organic components and grain-size distribution of cuttings, respectively. A special thanks goes to Fabian Horn (GFZ) for helping to process the DNA sequence data. The research was funded by the German Ministry of Energy and Economics (BMWi) within the research and demonstration project "Efficiency and safety of energy systems with seasonal energy storage in aquifers for urban quarters".

References

Alawi M, Lerm S, Vetter A, Wolfgramm M, Seibt A, Würdemann H (2011) Diversity of sulfate-reducing bacteria in a plant using deep geothermal energy. Grundwasser 16:105–112

Appelo CAJ, Postma D (2009) Geochemistry, groundwater and pollution, 2. Aufl. A.A. Balkema, Leiden

Banzhaf S, Krein A, Scheytt T (2013) Using selected pharmaceutical compounds as indicators for surface water and groundwater interaction in the hyporheic zone of a low permeability riverbank. Hydrol Process 27(20):2892–2902

Barth G, Franz M, Heunisch C, Wolfgramm M (2013) Deep geothermal reservoirs of the Lower Exter Formation (Upper Keuper, Triassic) in the North German Basin: the geothermal potential of distributive fluvial systems. DMG-Gv Meeting Tübingen, abstract volume

Bauer D, Marx R, Nußbicker-Lux J, Ochs F, Heidemann W, Müller-Steinhagen H (2010) German central solar heating plants with seasonal heat storage. Sol Energy 84(4):612–623

Beech IB, Sunner J (2004) Biocorrosion towards understanding interactions between biofilms and metals. Curr Opin Biotechnol 15:181–186

Beyer W (1964) Zur Bestimmung der Wasserdurchlassigkeit von Kiesen und Sanden aus der ornverteilung. Wasserwirtschaft Wassertechnik (WWT) 6:165–169

Birsoy YK, Summers WK (1980) Determination of aquifer parameters from step tests and intermittent pumping data. Groundwater 18(2):137–146

Caporaso JG, Kuczynski J, Stombaugh J, Bittinger K, Bushman, FD & other authors (2010) QIIME allows analysis of high-throughput community sequencing data. Nat Methods 7:335–336

Caporaso JG, Lauber CL, Walters WA, Berg-Lyons D, Lozupone CA, Turnbaugh PJ, Fierer N, Knight R (2011) Global patterns of 16S rRNA diversity at a depth of millions of sequences per sample. Proc Natl Acad Sci 108: 4516–4522. https://doi.org/10.1073/pnas.1000080107

Cummings DE, Caccavo F Jr, Spring S, Rosenzweig RF (1999) *Ferribacterium limneticum*, gen. nov., sp. nov., an Fe(III)-reducing microorganism isolated from mining-impacted freshwater lake sediments. Arch Microbiol 171:183–188

DVGW, Deutscher Verein des Gas- und Wasserfaches (1998) Verwendung von Spülungszusätzen in Bohrspülungen bei Bohrarbeiten im Grundwasser. DVGW-Regelwerk, Merkblatt 116, Bonn

Edgar RC (2010) Search and clustering orders of magnitude faster than BLAST. Bioinformatics 26(19):2460–2461

Feldbusch E, Regenspurg S, Banks J, Milsch H, Saadat A (2013) Alteration of fluid properties during the initial operation of a geothermal plant: results from in situ measurements in Groß Schönebeck. Environ Earth Sci 70(8):3447–3458

Filippidou S, Jaussi M, Junier T, Wunderlin T, Jeanneret N, Palmieri F et al (2016) *Anoxybacillusgeothermalis* sp. nov., a facultatively anaerobic, endospore-forming bacterium isolated from mineral deposits in a geothermal station. International journal of systematic evolutionary microbiology 66(8):2944–2951

Geets J, Borremans B, Diels L, Springael D, Vangronsveld J, van der Lelie D, Vanbroekhoven K (2006) DsrB gene-based DGGE for community and diversity surveys of sulfate-reducing bacteria. J Microbiol Methods 66:194–205. https://doi.org/10.1016/j.mimet.2005.11.002

Hammer Ø, Harper DAT, Ryan PD (2001) PAST—palaeontological statistics, ver. 1.89. Palaeontol Electron 4(1):1–9

Huber SA, Balz A, Abert M, Pronk W (2011) Characterisation of aquatic humic and non-humic matter with size-exclusion chromatography–organic carbon detection–organic nitrogen detection (LC–OCD–OND). Water Res 45(2):879–885

Javerhadashti R (2008) Microbiologically influenced corrosion. An engineering insight. Springer, London

Kabus F, Wolfgramm M, Seibt A, Richlak U, Beuster H (2009) Aquifer thermal energy storage in Neubrandenburg: monitoring throughout three years of regular operation. In Proceedings of the 11th international conference on energy storage

Käss W (2004) Geohydrologische Markierungstechnik: Mit 43 Tabellen. XIV, 557 S.In. In: Lehrbuch der Hydrogeologie, Bd. 9, 2. Aufl. Borntraeger, Stuttgart

Krauze P, Kämpf H, Horn F, Liu Q, Voropaev A, Wagner D, Alawi M (2017) Microbiological and geochemical survey of CO_2-dominated mofette and mineral waters of the Cheb Basin, Czech Republic. Front Microbiol 8:2466. https://doi.org/10.3389/fmicb.2017.02446

Langguth HR, Voigt R (2004) Hydrogeologische Methoden. xiv, 1005, 2. Aufl. Springer, Berlin

Lee KS (2013) Aquifer thermal energy storage. In: Underground thermal energy storage. Springer, London, pp 59–93

Lerm S, Alawi M, Miethling-Graff R, Wolfgramm M, Rauppach K, Seibt A, Würdemann H (2011) Influence of microbial processes on the operation of a cold store in a shallow aquifer: impact on well injectivity and filter lifetime. Grundwasser 16(2):93–104

Little BJ, Lee JS (2007) Microbiologically influenced corrosion. Wiley, Hoboken

Magal E, Weisbrod N, Yakirevich A, Yechieli Y (2008) The use of fluorescent dyes as tracers in highly saline groundwater. J Hydrol 358:124–133

Martin M (2011) Cutadapt removes adapter sequences from high-throughput sequencing reads. EMBnet J 17(1):10

McCaughey M, Divine CE, Gefell MJ, McGrane S (2016) Using tracers to quantify drilling water influence and obtain representative groundwater samples. Groundw Monit Remediat 36(1):71–78

Morozova D, Wandrey M, Zimmer M, Pilz P, Zettlitzer M, Würdemann H, the CO2SINK Group (2010) Monitoring of the microbial community composition in saline aquifers during CO_2 sequestration by fluorescence in situ hybridisation. Int J Greenh Gas Control 4:981–989. https://doi.org/10.1016/j.ijggc.2009.11.014

Müller D, Regenspurg S (2014) Geochemical characterization of the Lower Jurassic aquifer in Berlin (Germany) for aquifer thermal energy storage applications. Energy Procedia 59:285–292

Müller DR, Friedland G, Regenspurg S (2017) An improved sequential extraction method to determine element mobility in pyrite-bearing siliciclastic rocks. Int J Environ Anal Chem 97(2):168–188

Mundhenk N, Huttenloch P, Sanjuan B, Kohl T, Steger H, Zorn R (2013) Corrosion and scaling as interrelated phenomena in an operating geothermal power plant. Corros Sci 70:17–28

Nadkarni MA, Martin FE, Jacques NA, Hunter N (2002) Determination of bacterial load by real-time PCR using a broad-range (universal) probe and primers set. Microbiology 148:257–266

Paksoy H, Snijders A, Stiles L (2009) State-of-the-art review of aquifer thermal energy storage systems for heating and cooling buildings. In: Proceedings of the EFFSTOCK conference, Stockholm, Sweden

Parkhurst DL, Appelo CAJ (1999) User's guide to PHREEQC (version 2): a computer program for speciation, batch-reaction, one-dimensional transport, and inverse geochemical calculations

Pellizzari L, Neumann D, Alawi M, Voigt D, Norden B, Würdemann H (2013) Use of tracers to assess drill mud penetration depth into sandstone rock cores during deep drilling: method development and application. Environ Earth Sci 70:3727–3738. https://doi.org/10.1007/s12665-013-2715-2

Pellizzari L, Lienen T, Kasina M, Würdemann H (2017) Influence of drill mud on the microbial communities of sandstone rocks and well fluids at the Ketzin pilot site for CO_2 storage. Environ Earth Sci. https://doi.org/10.1007/s12665-016-6381-z

Quast C, Pruesse E, Yilmaz P, Gerken J, Schweer T, Yarza P et al (2013) The SILVA ribosomal RNA gene database project: improved data processing and web-based tools. Nucleic Acids Res 41(Database issue):D590–D596. pmid:23193283

Regenspurg S, Feldbusch E, Byrne J, Deon F, Driba DL, Henninges J, Kappler A, Naumann R, Reinsch T, Schubert C (2015) Mineral precipitation during production of geothermal fluid from a Permian Rotliegend reservoir. Geothermics 54:122–135

Regenspurg S. Feldbusch E, Norden B, Tichomirowa M (2016) Fluid–rock interactions in a geothermal Rotliegend/Permo-Carboniferous reservoir (North German Basin). Appl Geochem 69:12–27

Robertson WJ, Bowman JP, Franzmann PD, Mee BJ (2001) *Desulfosporosinus meridiei* sp. nov., a spore-forming sulfatereducing bacterium isolated from gasolene-contaminated groundwater. Int J Syst Evol Microbiol 51:133–140

Rozanova EP, Nazina TN, Galushko AS (1988) Isolation of a new genus of sulfate-reducing bacteria and the description of its new species *Desulfomicrobium apsheromum* gen, nov., sp. nov. Mikrobiologiya 57:514–520

Saadat A, Blöcher G, Francke H, Huenges E, Kranz S, Kupfermann A, Norden B, Regenspurg S (2016) Effizienz und Betriebssicherheit von Energiesystemen mit saisonaler Energiespeicherung in Aquiferen für Stadtquartiere. FKZ 03ESP409A. Abschlussbericht des Teilprojekts "Gesamtsystem"

Sanner B, Kabus F, Seibt P, Bartels J (2005) Underground thermal energy storage for the German Parliament in Berlin, system concept and operational experiences. In Proceedings world geothermal congress, vol 1, pp 1–8

Schneider J, Eggeling L, Hesshaus A (2014) Tiefengrundwassercharakteristik und hydrochemische Untersuchung. In: Bauer M, Freeden W, Jacobi H, Neu T (Hrsg) Handbuch Tiefe Geothermie: Prospektion, Exploration, Realisierung, Nutzung. Springer Spektrum, Berlin, pp 559–594

Schouw A, Leiknes Eide T, Stokke R, Birger Pedersen R, Helene Steen I, Bodtker G (2016) *Abyssivirga alkaniphila* gen. nov., sp. nov., an alkane-degrading, anaerobic bacterium from a deep-sea hydrothermal vent system, and emended descriptions of *Natranaerovirga pectinivora* and *Natranaerovirga hydrolytica*. Int J Syst Evol Microbiol 66:1724–1734

Seelheim F (1880) Methoden zur Bestimmung der Durchlässigkeit des Bodens. Zeitschrift für analytische Chemie 19(1):387–418

Steinberg LM, Regan JM (2009) mcrA-targeted real-time quantitative PCR method to examine methanogen communities. Appl Environ Microbiol 75(13):4435–4442

Stober I, Bucher K (2014) Geothermie. Online-Ressource (online resource), 2. Aufl. Springer Spektrum, Berlin **(SpringerLink: Bücher)**

Stober I, Wolfgramm M, Birner J (2014) Hydrochemie der Tiefenwässer in Deutschland. Zeitschrift für geologische Wissenschaften 41(42):339–380

Struchtemeyer CG, Davis JP, Elshahed MS (2011) Influence of the drilling mud formulation process on the bacterial communities in thermogenic natural gas wells of the Barnett shale. Appl Environ Microbiol 77(14):4744–4753

Takai K, Abe M, Miyazaki M, Koide O, Nunoura T, Imachi H, Inagaki F, Kobayashi T (2013) Sunxiuqinia faeciviva sp. nov., a facultatively anaerobic organoheterotroph of the Bacteroidetes isolated from deep subseafloor sediment. Int J Syst Evol Microbiol 63:1602–1609

Theis CV (1935) The relation between the lowering of the Piezometric surface and the rate and duration of discharge of a well using ground-water storage. Eos Trans Am Geophys Union 16(2):519–524

Wagner M, Roger AJ, Flax JL, Brusseau GA, Stahl DA (1998) Phylogeny of dissimilatory sulfite reductases supports an early origin of sulfate respiration. J Bacteriol 180:2975–2982

Wiese B, Zimmer M, Nowak M, Pellizzari L, Pilz P (2013) Well-based hydraulic and geochemical monitoring of the above zone of the CO_2 reservoir at Ketzin, Germany. Environ Earth Sci 70(8):3709–3726

Wolfgramm M, Thorwart K, Rauppach K, Brandes J (2011) Zusammensetzung, Herkunft und Genese geothermaler Tiefengrundwässer im Norddeutschen Becken (NDB) und deren Relevanz für die geothermische Nutzung. Zeitschrift für geologische Wissenschaften 39(3–4):173.193

Zhang MY, Fan L, Liu QZ, Song Y, Wei SW, Zhang SL, Wu J (2014) A novel set of EST-derived SSR markers for pear and cross-species transferability in Rosaceae. Plant Mol Biol Rep 32(1):290–302

Zhu Y, Vieth-Hillebrand A, Wilke FD, Horsfield B (2015) Characterization of water-soluble organic compounds released from black shales and coals. Int J Coal Geol 150:265–275